

---

## Water-soluble poly(3-hydroxyalkanoate) sulfonate: versatile biomaterials used as coatings for highly porous nano-MOF

Jain Caroline <sup>1,2</sup>, Li Xue <sup>3</sup>, Houel Renault Ludivine <sup>4</sup>, Modjinou Tina <sup>1</sup>, Simon Colin Christelle <sup>2</sup>, Gref Ruxandra <sup>3</sup>, Renard Estelle <sup>1</sup>, Langlois Valérie <sup>1,\*</sup>

<sup>1</sup> Institut de Chimie et des Matériaux Paris-Est, UPEC-CNRS, 2 rue Henry Dunant, 94320 Thiais, France

<sup>2</sup> Ifremer, UMR 6197, Laboratoire de Microbiologie des Environnements Extrêmes (LM2E), Technopôle Pointe du Diable, 29280 Plouzané, France

<sup>3</sup> Institut des Sciences Moléculaires d'Orsay, UMR 8214, CNRS-UPS, Rue André Rivière, 91405 Orsay, France

<sup>4</sup> Centre Laser de l'Université Paris-Sud (CLUPS/LUMAT), CNRS-UPS-IOGS, Université Paris-Saclay, 91405 Orsay, France

\* Corresponding author : Valérie Langlois, email address : [langlois@icmpe.cnrs.fr](mailto:langlois@icmpe.cnrs.fr)

---

### Abstract :

Water soluble poly(3-hydroxyalkanoate) containing ionic groups was designed by two successive photo-activated thiol-ene reactions. Sodium-3-mercaptopropionate (SO<sub>3</sub><sup>-</sup>) and poly(ethylene glycol) methyl ether thiol (PEG) were grafted onto poly(3-hydroxyoctanoate-co-3-hydroxyundecenoate) PHO(67)U(33) to both introduce ionic groups and hydrophilic moieties. The grafted copolymers PHO(67)SO<sub>3</sub>-(20)PEG(13) were then used as biocompatible coatings of nano-Metal Organic Frameworks surface. Scanning Electron Microscopy and Scanning Transmission Electron Microscopy coupled with Energy Dispersive X-ray characterizations have clearly demonstrated the presence of the copolymer on the MOF surface. These coated nano-MOF are stable in aqueous and physiological fluids. Cell proliferation and cytotoxicity tests performed on murine macrophages J774.A1 revealed no cytotoxic side effect. Thus, biocompatibility and stability of these novel hybrid porous MOF structures encourage their use in the development of effective therapeutic nanoparticles.

**Keywords :** Polyhydroxyalkanoates, PHOU, thiol-ene photoactivated, PEG, MOF, nanoparticles

## 1. INTRODUCTION

Poly(3-hydroxyalkanoates) (PHAs) are biodegradable polymers synthesized by many organisms, especially prokaryotes. There are over 150 types of these polyesters, accumulated as carbon and energy storage material in a wide variety of bacteria. PHA granules are produced when microorganisms are cultivated in the presence of both carbon source excess and nitrogenous nutrient deficiency.<sup>1-2</sup> According to the length of side chains, different types of PHAs can be classified as either a short chain length, scl-PHAs, a medium chain length, mcl-PHAs and lcl-PHA, long chain length. Physical properties are related to the length of these side chain; thus, scl-PHAs are semi-crystalline, rigid and brittle whereas mcl-PHAs are soft and elastomeric.

Over the last three decades, biomaterials based on PHAs have been developed for medical or pharmaceutical applications<sup>3-12</sup> such as tissue engineering, implants or drug delivery carriers due to their proven biodegradability, biocompatibility and lack of toxicity. In order to enlarge the potential in biomedical applications, many chemical modifications have been developed. Among them, the combination of the properties of hydrophobic PHA and hydrophilic PEG was used to prepare amphiphilic PHAs. The excellent water-solubility and biocompatibility of PEG, encouraging the use of this polymer in biomedical applications.<sup>13-15</sup> Moreover PEG having molar mass in the range of 2,000-5,000 g/mole confers a long blood-circulation ability by reducing both nanoparticles accumulation in liver and spleen, and mononuclear phagocyte system uptake (stealth behaviour),<sup>16</sup> in order to avoid *in vivo* nanoparticles rapid elimination. Micro- and nanoparticles based on amphiphilic PHA-block-PEG copolymer have been extensively studied as drug delivery system.<sup>17-28</sup> PEGylation of PHAs can be performed by chemical modifications or by bioprocessing *in vivo*, bioPEGylation. Regarding the chemical way, block copolymers were synthesized by direct transesterification or by using telechelic oligomers based on PHAs. A series of amphiphilic diblock and graft PEG-PHA copolymers were recently prepared through a click chemistry approach.<sup>21-22</sup> Another way to improve hydrophilicity or water-solubility of organic compound is to introduce ionic groups as carboxylic groups,<sup>29</sup> ammonium groups,<sup>30</sup> N-acetyl-L-lysine<sup>31</sup> and sulfonate functions.<sup>32</sup> The sulfonate anionic sites are known to display biological interactions and they can interact with proteins.<sup>33</sup> A series of PHAs sulfonate have been prepared using the highly versatile approach as photoactivated thiol-ene or thiol-yne reactions. These new amphiphilic scl-PHAs oligomers were able to self-assemble in aqueous solution whereas the sulfonate derivatives of mcl-PHAs are totally soluble in water if the content of sulfonate groups is superior to 25% whatever the molar mass of the PHAs.<sup>32</sup> In this context, we used here the large versatility of the thiol-ene

1  
2  
3 72 reaction to introduce both sulfonate groups and PEG grafts. It has already been demonstrated  
4  
5 73 that the PHAs having unsaturated groups in the side chains are very useful to introduce reactive  
6  
7 74 groups by using thiol-ene reactions. Poly(3-hydroxyoctanoate-co-3-hydroxyundecenoate)  
8  
9 75 PHO<sub>(67)</sub>U<sub>(33)</sub> is a functionalized mcl-PHA bearing molar ratio 33% of terminal alkene units on  
10  
11 76 its side chains. First, thiol containing sulfonate groups were reacted with unsaturated PHAs. In  
12  
13 77 a second step, the PEG grafting was achieved *via* a similar thiol-ene addition, which has proven  
14  
15 78 to be an effective reaction to chemical modify the unsaturated PHAs.<sup>22,31,34</sup>  
16  
17 79 The objective here was to propose a versatile biodegradable and biocompatible polymeric  
18  
19 80 coating for highly porous nanosized metal organic frameworks (nanoMOFs). NanoMOFs,  
20  
21 81 formed by strong coordination between metal ions and organic ligands, recently emerged in the  
22  
23 82 world of therapeutic nanovectors.<sup>35-39</sup> In particular, iron trimesate nanoMOFs MIL-100(Fe)  
24  
25 83 (MIL stands for Material from Institut Lavoisier) have large surface areas allowing to load a  
26  
27 84 large variety of drugs able to penetrate within the porous MOF structures.<sup>40-41</sup> These porous  
28  
29 85 solids are built up from Fe(III) octahedra trimers and trimesate linkers (1,3,5-benzene  
30  
31 86 tricarboxylate) that self-assemble to build a porous architecture delimiting large (29 Å) and  
32  
33 87 small (24 Å) mesoporous cages. The two types of cages are accessible for drug adsorption inside  
34  
35 88 the 3D-porosity through pentagonal (5.6 Å) and hexagonal windows (8.6 Å). Due to the  
36  
37 89 presence of Fe and free water molecules in their structure, they acted as efficient T<sub>2</sub>-weighted  
38  
39 90 contrast agents for Magnetic Resonance Imaging (MRI) of interest for theranostics.<sup>42</sup> The lack  
40  
41 91 of toxicity of MIL-100(Fe) nanoMOFs has been established *in vivo* after repetitive  
42  
43 92 administrations.<sup>43-45</sup> These materials offer a particular hydrophilic/hydrophobic  
44  
45 93 microenvironment inside their open porosity, allowing the incorporation of a large variety of  
46  
47 94 either water-soluble or hydrophobic active molecules, by simple one-step impregnation,  
48  
49 95 generally without organic solvent.<sup>41-42</sup>  
50  
51 96 For last five years, there has been an intensive research in coating nanoMOFs in order to prevent  
52  
53 97 premature drug release, improve colloidal stability, and control the *in vivo* fate. For instance,  
54  
55 98 oligomers or polysaccharides (cyclodextrin, heparin, hyaluronic acid or chitosan),<sup>43,44,46-49</sup>  
56  
57 99 dioleoyl-phosphocholine lipid<sup>50</sup> or polycaprolacton<sup>51</sup> were used. Of main interest, PEG grafting  
58  
59 100 onto MOF nanoparticles surface was also performed to generate stealth material against  
60  
61 101 immune system.<sup>43,52-54</sup> We here developed a new hybrid system, composed of nanoporous  
62  
63 102 MIL-100(Fe) nanoMOF coated by a water-soluble PEGylated PHA containing sulfonate groups  
64  
65 103 that should be able to strongly interact with nanoMOF. Thus, all or part of PHOU lateral  
66  
67 104 unsaturations were first functionalized with SO<sub>3</sub><sup>-</sup> and PEG groups, in order to improve water-  
68  
69 105 solubility and achieve efficient PEG grafting as well as metal interactions between

1  
2  
3 106 functionalized PHA and MOF. Then, MOF-PHA hybrid nanoparticles were synthesized by a  
4  
5 107 rapid one-step non-covalent method or impregnation, and their structure was investigated by  
6  
7 108 complementary physicochemical methods. More particularly, for the first time, scanning  
8  
9 109 transmission electron microscopy (SEM-STEM) using energy dispersive X-ray (EDX)  
10  
11 110 spectroscopy was used to unravel the structure of the coated nanoMOFs and enable gaining  
12  
13 111 information on the coating location. Cell proliferation and cytotoxicity tests were carried out  
14  
15 112 on murine J774.A1 macrophages to evaluate MOF-PHA hybrid porous nanoparticles toxicity.  
16  
17 113

## 18 114 2. MATERIALS AND METHODS

### 19 115 20 116 2.1. Materials

21  
22  
23 117 Dimethyl sulfoxide (DMSO), methanol (MeOH) and tetrahydrofuran (THF) were obtained  
24  
25 118 from VWR International. 2,2-dimethoxy-2-phenylacetophenone (DMPA), sodium-3-mercapto-  
26  
27 119 1-ethanesulfonate ( $\text{SO}_3^-$ ), poly(ethylene glycol) methyl ether thiol (PEG, molar mass: 2,000  
28  
29 120  $\text{g}\cdot\text{mol}^{-1}$ ) were purchased from Sigma Aldrich. Dialysis membranes (MWCO 1 and 6-8 KDa)  
30  
31 121 were procured from Spectrumlabs. Poly(3-hydroxyoctanoate-co-3-hydroxyundecenoate)  
32  
33 122  $\text{PHO}_{(67)}\text{U}_{(33)}$  was provided from HES-SO Valais-Wallis, Switzerland.  
34  
35 123

### 36 124 2.2. Synthesis of $\text{PHO}_{(67)}\text{U}_{(13)}\text{SO}_3^-(20)$

37 125 100 mg of  $\text{PHO}_{(67)}\text{U}_{(33)}$  ( $M_n = 40,000 \text{ g/mol}$ ,  $2.13 \times 10^{-4} \text{ mol C=C}$ ) and 0.2 eq of photoinitiator  
38  
39 126 DMPA/C=C were dissolved in 6 mL of THF (Solution 1). On the other hand, 1.2 eq of  $\text{SO}_3^-$   
40  
41 127 /C=C were solubilized in 6 mL of MeOH then adding 3 mL of THF drop by drop (Solution 2).  
42  
43 128 Solution 2 was mixed with the first and the resulting mixture was irradiated during 10 min at  
44  
45 129 room temperature by Lightning cure LC8 (L8251, Hamamatsu) equipped with a mercury-xenon  
46  
47 130 lamp ( $180 \text{ mW}\cdot\text{cm}^{-2}$ ) coupled with a flexible light guide whose end was placed 11 cm from the  
48  
49 131 sample. At last, 30 mL of DMSO were added to the resultant solution before purification by  
50  
51 132 dialysis (MWCO 1,000 Da) against 2 L of water for 2 days with 4 water changes per day,  
52  
53 133 followed by freeze-drying (yield 86%).  
54  
55 134

### 56 135 2.3. Synthesis of $\text{PHO}_{(67)}\text{U}_{(7)}\text{SO}_3^-(20)\text{PEG}_{(6)}$ and $\text{PHO}_{(67)}\text{SO}_3^-(20)\text{PEG}_{(13)}$

57 136 50 mg of  $\text{PHO}_{(67)}\text{U}_{(13)}\text{SO}_3^-(20)$  were dissolved in DMSO at a concentration of 16.7 g/L before  
58  
59 137 adding 3 eq (for copolymer containing  $\text{PEG}_{(6)}$ ) or 8 eq (for copolymer containing  $\text{PEG}_{(13)}$ ) of  
60  
138  $\text{PEG/C=C}$  and 0.2 eq of DMPA/C=C. The mixture was then irradiated during 30 min at a

1  
2  
3 139 distance of 11 cm prior purification. Next, copolymer was diluted at 2 g/L in DMSO before  
4  
5 140 dialysis against 2 L of water in 6-8 KDa MWCO membrane during 3 days with 4 water changes  
6  
7 141 per day, followed by freeze-drying. Manipulation was repeated 4 times until maximal  
8  
9 142 elimination of excess PEG (yields of 90 and 94%, respectively).

10 143

#### 11 144 **2.4. Characterization**

12  
13 145 <sup>1</sup>H NMR spectra were recorded in CDCl<sub>3</sub> or DMSO-d<sub>6</sub> on a Bruker AV400 MHz. Size  
14  
15 146 exclusion chromatography (SEC) experiments were determined in chloroform for PHOU using  
16  
17 147 Shimadzu LC-10AD pump with two Shodex GPC K-805L columns (5 μm Mixte-C) or in  
18  
19 148 LiNO<sub>3</sub>·0.5 M solution for copolymers using two PL aquagel-OH 40-30 columns (8 μm Mixte-  
20  
21 149 C), both at a concentration of 10 mg/mL. A Wyatt Technology Optilab Rex interferometric  
22  
23 150 refractometer was used as detector, and low polydispersity index polystyrene standards (3 × 10<sup>4</sup>  
24  
25 151 - 2 × 10<sup>6</sup> g/mol) for PHOU analysis, or PEO standards (polyethylene oxide, 106 - 4.6 × 10<sup>4</sup> g/mol)  
26  
27 152 for copolymers measurements, were used to calibrate the system. Differential scanning  
28  
29 153 calorimetry (DSC) measurements were performed on a Perkin Elmer Diamond DSC apparatus.  
30  
31 154 The following protocol was used for each sample: heating from -60 to +200 °C at 10 °C/min,  
32  
33 155 cooling to -60 °C at 200 °C/min, hold 5 min and heat again to 200 °C at 10 °C/min.

34  
35 156 Transmittance measurements were performed on a Cary50 Bio Varian UV-Visible  
36  
37 157 spectrophotometer controlled by Cary Win UV software. The acquisition was performed from  
38  
39 158 250 to 800nm. A 1g.L<sup>-1</sup> solution of PHO<sub>(67)</sub>U<sub>(7)</sub>SO<sub>3</sub><sup>-</sup>(<sub>20</sub>)PEG<sub>(6)</sub> in ultrapure water was used to  
40  
41 159 evaluate the solubility properties of the copolymer. The transmittance of this solution was  
42  
43 160 measured using ultrapure water as reference for the 100% of transmittance.

44 161

#### 45 162 **2.5. Preparation of MOF-PHA nanoparticles**

46  
47 163 MIL-100(Fe) iron-carboxylate nanoMOF were synthesized by microwave assisted  
48  
49 164 hydrothermal reaction as previously described.<sup>38,43</sup> 1 mg (40 μL) of MOF was modified by  
50  
51 165 impregnation with PHO<sub>(67)</sub>U<sub>(7)</sub>SO<sub>3</sub><sup>-</sup>(<sub>20</sub>)PEG<sub>(6)</sub> or PHO<sub>(67)</sub>SO<sub>3</sub><sup>-</sup>(<sub>20</sub>)PEG<sub>(13)</sub> (from 17 to 83% (w/w))  
52  
53 166 in a final MilliQ water volume of 500 μL (MOF final concentration 2 mg/mL) under gentle  
54  
55 167 rotative agitation for 1 h at room temperature in the dark.

56 168

#### 57 169 **2.6. Characterization by STEM-EDX and TEM-EDX**

58  
59 170 PHA-MOF nanoparticles size and surface charge were measured by dynamic light scattering  
60  
171 (DLS) and zeta potential (ZP) on a Malvern Zetasizer Nano ZS. PHA-MOF nanoparticles

1  
2  
3 172 morphology was investigated by transmission electron microscopy (TEM) on a JEOL-2100F  
4 173 microscope operating at 200 KV. Chemical composition was investigated with a FEI TECNAI  
5 174 G2 F20 equipped with scanning TEM (STEM) device fitted to high angle annular dark field  
6 175 imaging (HAADF), energy dispersive X-ray spectrometer (EDX) and electron energy-loss  
7 176 spectrometer (EELS). Chemical composition was also performed with a Merlin (Carl Zeiss)  
8 177 equipped with an EDX Advanced SDD X-Max detector (Oxford Instruments).  
9  
10  
11  
12  
13  
14

## 15 179 **2.7. Cell culture**

16  
17 180 Murine macrophages J774.A1 adherent cells were grown at 37 °C under humidified atmosphere  
18 181 with 5% CO<sub>2</sub> in Dulbecco's Modified Eagle Medium (DMEM) GlutaMAX™ supplemented  
19 182 with 10% inactivated fetal bovine serum, penicillin G (100 U/mL) and streptomycin (0.1  
20 183 mg/mL). During experiments, medium was exchanged three times per week.  
21  
22  
23  
24

## 25 185 **2.8. Cytotoxicity assay**

26  
27 186 Into 96 well plate, J774.A1 were seeded at 20,000 cells/well and then 25, 50, 100, 200 or 400  
28 187 µg/mL of uncoated MOF, copolymers of PHA grafted with 6 or 13% of PEG and MOF-PHA  
29 188 nanoparticles were added following the manufacturer's protocols (LDH cytotoxicity assay,  
30 189 Roche). After 24h incubation at 37 °C, absorbance was measured with a Clariostar microplate  
31 190 reader (excitation at 490 nm and emission at 680 nm). As a positive control, cells were exposed  
32 191 to medium containing sterile MilliQ water while untreated murine macrophages served as  
33 192 negative control.  
34  
35  
36  
37  
38

## 39 193 40 194 **2.9. Cell proliferation assay**

41  
42 195 Into 96 wells plate, J774.A1 were seeded at 5,000 cells/well and then 25, 50 or 100 µg/mL of  
43 196 uncoated MOF, copolymers of PHA grafted with 6 or 13% of PEG and MOF-PHA  
44 197 nanoparticles were added following the manufacturer's protocols (RealTime-Glo™ MTT Cell  
45 198 Viability Assay kit, Promega). After 72h incubation at 37 °C, bioluminescence intensity was  
46 199 measured every day with a Glomax microplate reader. As a negative control, cells were exposed  
47 200 to medium containing sterile MilliQ water while untreated murine macrophages served as  
48 201 positive control.  
49  
50  
51  
52  
53  
54

## 55 202 56 203 **3. RESULTS AND DISCUSSION**

### 204 **3.1. Preparation and characterization of poly(3-hydroxyalkanoate) sulfonate grafted with** 205 **PEG**

206 Poly(3-hydroxyoctanoate-co-3-hydroxyundecenoate)  $\text{PHO}_{(67)}\text{U}_{(33)}$  is a hydrophobic polyester  
207 composed of long alkyl side chains and lateral alkene groups. The interest in preparing PHA-  
208 based copolymers that are both covalently grafted with PEG and sulfonate functions is twofold.  
209 It allows both to bind it to the nano-MOF surface by ionic interactions and to avoid the  
210 aggregation of nanoparticles due to hydrophilic PEG grafts whose modify the hydrodynamic  
211 volume of particles. These particles also became less detectable by immune system cells. First,  
212 sulfonate groups ( $\text{SO}_3^-$ ) were grafted to the terminal double bonds of the  $\text{PHO}_{(67)}\text{U}_{(33)}$ , not only  
213 to provide an amphiphilic character to the material,<sup>32</sup> but also to induce non-covalent binding  
214 of  $\text{SO}_3^-$  ions to  $\text{Fe}^{3+}$  ions that are present on the surface of MOF-type nanoparticles, by simple  
215 impregnation as shown in Figure 1.  $\text{PHO}_{(67)}\text{U}_{(33)}$  was characterized by  $^1\text{H}$  NMR (Figure 2) to  
216 determine the percentage of terminal unsaturations by integrating protons corresponding to the  
217 CH peak (2) at 5.1 ppm, and the signal relating to the terminal alkene group of side chain (7) at  
218 5.7 ppm. Sodium-3-mercapto-1-ethanesulfonate was grafted under photochemical activation,  
219 using from 1 to 5 molar equivalents of sulfonates ( $\text{SO}_3^-$ ). After purification by dialysis,  
220 polymers were analyzed by  $^1\text{H}$  NMR, and signals relating to the two  $\text{CH}_2$  methylenes (c, d),  
221 characteristic of sulfonate groups, appear at 2.66 ppm, indicating the success of the grafting.  
222 The conversion percentages of the terminal double bonds to  $\text{SO}_3^-$  were calculated by comparing  
223 the integrations of the protons corresponding to the CH peak (2) of the  $\text{PHO}_{(67)}\text{U}_{(33)}$  structure at  
224 5.1 ppm, with respect to the signal of terminal unsaturation HU side chain (7) at 5.7 ppm (Figure  
225 3). The results obtained indicate a non-linear relationship between the conversion rate of double  
226 bonds of  $\text{PHO}_{(67)}\text{U}_{(33)}$  and the concentrations of sodium-3-mercapto-1-ethanesulfonate (RSH)  
227 used. The copolymers were obtained with yields between 86 and 95%, reflecting the  
228 effectiveness of the grafting method. In order to maintain a sufficient number of unsaturations  
229 for the subsequent grafting of PEG methyl ether thiol,  $\text{PHO}_{(67)}\text{U}_{(13)}\text{SO}_3^-(20)$  is therefore obtained  
230 by using 1.2 equivalents  $\text{RSH}/\text{C}=\text{C}$ . The copolymer is not soluble in water, THF or even  $\text{CHCl}_3$   
231 as it is traditionally the case with native PHA whereas complete solubilization is observed in  
232 DMSO.

233 In a second step PEG methyl ether thiol was grafted using the photoinduced thiol-ene reaction.  
234 Low molecular weight PEG is a highly polar and water-soluble polymer, widely used in  
235 pharmaceuticals for its biocompatibility and stealth properties. Two different ratios of PEG  
236 methyl ether thiol (3 and 8 molar equivalents of PEG per mole of PHOU unsaturation) were  
237 used (Figure 4). Two peaks are observed at 3.5 and 3.2 ppm, corresponding to the  $\text{CH}_2$  (e) and

1  
2  
3 238 CH<sub>3</sub> (f) methyl terminal groups of the PEG confirming the success of the grafting. The grafting  
4  
5 239 percentages were calculated from the integrations of the signals of the PHOU at 5.1 ppm, and  
6  
7 240 the signal relating to the terminal unsaturations of the HU pattern side chain (7) at 5.7 ppm.  
8  
9 241 Two PEG ratios were found attesting the synthesis of copolymers of PHO<sub>(67)</sub>U<sub>(7)</sub>SO<sub>3</sub><sup>-</sup><sub>(20)</sub>PEG<sub>(6)</sub>  
10 242 with the use of 3 eq PEG/C=C, and PHO<sub>(67)</sub>SO<sub>3</sub><sup>-</sup><sub>(20)</sub>PEG<sub>(13)</sub> in presence of 8 eq PEG/C=C with  
11  
12 243 a yield of 92%. The turbidity measurement showed a colorless solution at 550 nm indicating  
13  
14 244 absence of micelles or aggregates attesting of a total solubilization of HO<sub>(67)</sub>U<sub>(7)</sub>SO<sub>3</sub><sup>-</sup><sub>(20)</sub>PEG<sub>(6)</sub>  
15 245 and PHO<sub>(67)</sub>SO<sub>3</sub><sup>-</sup><sub>(20)</sub>PEG<sub>(13)</sub> in water (Figure 5). PEG methyl ether thiol, PHO<sub>(67)</sub>U<sub>(33)</sub> and the  
16  
17 246 copolymers of PHO<sub>(67)</sub>U<sub>(7)</sub>SO<sub>3</sub><sup>-</sup><sub>(20)</sub>PEG<sub>(6)</sub> and PHO<sub>(67)</sub>SO<sub>3</sub><sup>-</sup><sub>(20)</sub>PEG<sub>(13)</sub> were analyzed by SEC  
18  
19 247 (Table 1). PEG methyl ether thiol has a molecular weight of 1,700 g.mol<sup>-1</sup> and native  
20  
21 248 PHO<sub>(67)</sub>U<sub>(33)</sub> has a molar mass of 40,000 g.mol<sup>-1</sup> with a polydispersity index of 1.7, a value  
22  
23 249 generally obtained is the case of natural PHAs. The copolymers of PHO<sub>(67)</sub>U<sub>(7)</sub>SO<sub>3</sub><sup>-</sup><sub>(20)</sub>PEG<sub>(6)</sub>  
24 250 and PHO<sub>(67)</sub>SO<sub>3</sub><sup>-</sup><sub>(20)</sub>PEG<sub>(13)</sub> have molar masses of 24,000 and 29,500 g.mol<sup>-1</sup> respectively. The  
25  
26 251 difference of molar masses are explained by the difference of the chain conformations of  
27  
28 252 PHO<sub>(67)</sub>U<sub>(33)</sub> and the grafted copolymers. Furthermore, the molar masses are expressed in PS  
29  
30 253 equivalent in the case of PHO<sub>(67)</sub>U<sub>(33)</sub> and in PEG equivalents in the case of grafted copolymers  
31  
32 254 Consequently, the difference between natural PHO<sub>(67)</sub>U<sub>(33)</sub> and grafted copolymers are due to  
33  
34 255 the difference of their solubility instead of a potential degradation of macromolecular chains. It  
35  
36 256 has been previously shown that thiol-ene reactions proceeded without any chain scission of  
37  
38 257 unsaturated PHAs.<sup>20</sup> DSC measurements confirm the semi-crystalline structure of the  
39  
40 258 copolymers (Figure 5). However, the values of the melting enthalpies of copolymers are lower  
41  
42 259 than that of the free PEG, thus showing some inhibitory action of PHA on the crystallization of  
43  
44 260 PEG, a phenomenon already observed in similar work carried out by Babinot *et al.*<sup>20</sup> Similarly,  
45  
46 261 the presence of PEG polymers prevents the crystallization of PHA.

### 262 263 **3.2. Characterization of nano-hybrid MOF by electron microscopy and energy dispersive** 264 **X-ray spectrometer**

265 Transmission electron microscopy (TEM) images were performed on the native MOF and the  
266 MOF-PHA hybrid nanoparticles, MOF-PHO<sub>(67)</sub>U<sub>(7)</sub>SO<sub>3</sub><sup>-</sup><sub>(20)</sub>PEG<sub>(6)</sub> and MOF-PHO<sub>(67)</sub>SO<sub>3</sub><sup>-</sup>  
267 <sub>(20)</sub>PEG<sub>(13)</sub>. The overlay of MOF-type nanoparticles by functionalized PHA does not impact  
268 either the morphology or the size of the nanoparticles since average diameters between 250 and  
269 300 nm have been measured (Figure 6). The proportions of C, O, Fe and S atoms were  
270 quantified by STEM-EDX and SEM-EDX techniques. The presence of sulphur atoms,

1  
2  
3 271 characteristic of the presence of functionalized PHA at the surface of the nanoMOF, was  
4  
5 272 detected on the surface of both types of hybrid nanoparticles at equivalent atomic percentages  
6  
7 273 from both techniques (0.8%) (Table 2). The average S/Fe ratios were calculated in a very similar  
8  
9 274 way using the two STEM-EDX and SEM-EDX techniques (0.13-0.16), corresponding to one  
10  
11 275 sulphur atom as a marker for functionalized copolymers for eight iron atoms belonging to MOF.  
12  
13 276 These results confirm the adsorption of functionalized PHA copolymers on the surface of MOF-  
14  
15 277 type nanoparticles. The increase in the C/Fe ratio is all the more significant when the percentage  
16  
17 278 of PEG is high within copolymers, corresponding to rates of 11.6, 12.9 and 15.1 (STEM-EDX),  
18  
19 279 and 8.5, 10 and 11.1 (SEM-EDX), before and after coating nanoMOFs with  $\text{PHO}_{(67)}\text{U}_{(7)}\text{SO}_3^-$   
20  
21 280  ${}_{(20)}\text{PEG}_{(6)}$  or  $\text{PHO}_{(67)}\text{SO}_3^-{}_{(20)}\text{PEG}_{(13)}$  copolymers.

281

### 282 3.3. Stability of nano-hybrid MOF in aqueous medium

283 The two copolymers previously described were used to coat MOF nanoparticles to develop  
284 stable porous MOF-PHA hybrid systems (Figure 1). The zeta potential measurements showed  
285 a highly electropositive charge of +23 mV for native MOF nanoparticles, and electronegative  
286 charges of -41 mV for  $\text{PHO}_{(67)}\text{U}_{(7)}\text{SO}_3^-{}_{(20)}\text{PEG}_{(6)}$  and -24 mV for  $\text{PHO}_{(67)}\text{SO}_3^-{}_{(20)}\text{PEG}_{(13)}$ .  
287 Different concentrations of  $\text{PHO}_{(67)}\text{U}_{(7)}\text{SO}_3^-{}_{(20)}\text{PEG}_{(6)}$  and  $\text{PHO}_{(67)}\text{SO}_3^-{}_{(20)}\text{PEG}_{(13)}$  from 0.4 to  
288 10 g/L were placed in ultrapure water in presence of 2 g/L MOF. An instantaneous decrease in  
289 zeta potential measured on the surface of MOF nanoparticles after contact with 1 g/L  
290 copolymers was observed (Figure 7) thus confirming the coverage of MOF by functionalized  
291 PHA copolymers. The diameter of the nanoparticles were measured by DLS (Figure 8). The  
292 dispersion in water of the nanoMOF native or coated with 0.4 or 1 g/L PHA was not stable and  
293 the particles agglomerated in 1 hour. Incubation of nanoMOF in the presence of low (0.4 or 1  
294 g/L) concentrations of functionalized PHA was not sufficient to generate optimal recovery to  
295 ensure the stability of nanoparticles over time. These results are in agreement with previous  
296 studies showing the instability of the same nanoMOFs in aqueous media.<sup>46</sup> In contrast, the use  
297 of 2 g/L of copolymers of  $\text{PHO}_{(67)}\text{U}_{(7)}\text{SO}_3^-{}_{(20)}\text{PEG}_{(6)}$  and  $\text{PHO}_{(67)}\text{SO}_3^-{}_{(20)}\text{PEG}_{(13)}$  successfully  
298 allowed the development of stable hybrid nanoparticles. While  $\text{MOF-PHO}_{(67)}\text{SO}_3^-{}_{(20)}\text{PEG}_{(13)}$   
299 nanoparticles diameters remained stable for more than three days,  $\text{MOF-PHO}_{(67)}\text{U}_{(7)}\text{SO}_3^-$   
300  ${}_{(20)}\text{PEG}_{(6)}$  diameters measured by DLS were heterogeneous, greater than 350 nm during the first  
301 48 hours, higher than the expected 270-300 nm. These data again reflect some aggregation of  
302 particles possibly by a bridging effect and, in fact, insufficient coverage of PHAs on the surface  
303 of MOFs to ensure steric stabilization. The best results in terms of stability in water were  
304 obtained with the use of 4 g/L PHA regardless of the copolymer ( $\text{PHO}_{(67)}\text{U}_{(7)}\text{SO}_3^-{}_{(20)}\text{PEG}_{(6)}$  or

1  
2  
3 305 PHO<sub>(67)</sub>SO<sub>3</sub><sup>-</sup>(<sub>20</sub>)PEG<sub>(13)</sub>) over a 72-hour period. Complementary experiments showed that MOF-  
4  
5 306 PHO<sub>(67)</sub>SO<sub>3</sub><sup>-</sup>(<sub>20</sub>)PEG<sub>(13)</sub> nanoparticles remained stable for more than 6 hours in PBS.  
6  
7 307

### 8 308 **3.4. Biological tests**

9  
10 309 Grafted functionalized PHAs by using thiol-ene reaction did not demonstrate any significant  
11  
12 310 toxicity on the basis of viability assays on two different cell lines, mouse fibroblast cells  
13  
14 311 (NIH/3T3) and murine macrophage cells (J774.A1).<sup>55</sup> In this context, the possible *in vitro* toxic  
15  
16 312 effects of the MOF-PHA hybrid nanoparticles were determined using the LDH cytotoxicity.  
17  
18 313 The murine phagocytic cells J774.A1 were selected for these studies because they are model  
19  
20 314 cells, commonly used in cell biology and immunology, genetically stable and particularly  
21  
22 315 reactive in the presence of pathogens.<sup>56</sup> At concentrations lower than 50 µg/mL functionalized  
23  
24 316 PHA copolymers do not appear to generate toxic reaction against J774.A1 macrophages, as cell  
25  
26 317 viabilities close to 100% were observed (Figure 9). However, at concentrations in the range of  
27  
28 318 100-200 µg/mL, a proliferative effect was observed. This trend could be explained by processes  
29  
30 319 such as immune stimulation of the J774.A1 macrophages, which will have to be further  
31  
32 320 investigated. Finally, the use of hybrid nanoparticles MOF-PHO<sub>(67)</sub>U<sub>(7)</sub>SO<sub>3</sub><sup>-</sup>(<sub>20</sub>)PEG<sub>(6)</sub> and  
33  
34 321 MOF-PHO<sub>(67)</sub>SO<sub>3</sub><sup>-</sup>(<sub>20</sub>)PEG<sub>(13)</sub> at concentrations between 25 and 100 µg/mL does not cause any  
35  
36 322 significant reaction from J774.A1 cells, since percentages of cell viability close to 100% were  
37  
38 323 observed. However, the administration of hybrid nanoparticles at higher doses results in a  
39  
40 324 decrease macrophage viability, ranging from 70 to 85% at 200 µg/mL. Thus, in view of further  
41  
42 325 *in vitro* investigations, the nanoMOF concentrations were limited to 100 µg/mL. The  
43  
44 326 proliferation of macrophage-type immune cells is a marker of phagocytic activation, a step  
45  
46 327 preceding the inflammatory response.<sup>57-58</sup> The division of J774.A1 cells at 25, 50 or 100 µg/mL  
47  
48 328 of functionalized PHAs and native or hybrid MOF-type nanoparticles was measured over 42 h.  
49  
50 329 The cell proliferation experiments were conducted using the RealTime Glo kit which allows  
51  
52 330 the quantification of living cells from the bioluminescence emitted from the luciferase substrate,  
53  
54 331 reduced by the enzymatic activity of any viable cell. Results obtained after 42 h incubation of  
55  
56 332 J774.A1 macrophages with 25, 50 or 100 µg/mL of bare or hybrid PHA copolymers or  
57  
58 333 nanoMOFs are shown in Figure 10. These results demonstrate cell proliferation of the J774.A1  
59  
60 334 macrophages in contact with iron-based MOFs and further studies will be necessary to decipher  
335 the involved mechanism. However these preliminary results showed that materials were not  
336 cytotoxic.  
337

### 3. CONCLUSION

An efficient and reproducible method for the synthesis of copolymers of water-soluble PHO<sub>(67)</sub>U<sub>(7)</sub>SO<sub>3</sub><sup>-</sup>(<sub>20</sub>)PEG<sub>(6)</sub> and PHO<sub>(67)</sub>SO<sub>3</sub><sup>-</sup>(<sub>20</sub>)PEG<sub>(13)</sub> has been developed by two successive photoactivated thiol-ene reactions. These two copolymers will be used for the coating of MOF-type nanoparticles. The graft copolymers based on unsaturated PHAs have been heterofunctionalized with on one hand the polar SO<sub>3</sub><sup>-</sup> sulfonate groups to promote ionic interactions with nanoMOF and on the other hand with PEG moieties to improve hydrophilicity. The molar composition of the copolymer is strictly controlled thanks to the efficiency of the thiol-ene reaction. The presence of sulphur detected by the STEM technique coupled with EDX attests to the effective coating of the MOF surface by the functionalized copolymers. The presence of PEG aims on the one hand to increase the stability of the system in a physiological environment and on the other hand to escape the phagocytic cells of the immune system. Moreover, nano-hybrid MOF based on PHA copolymers do not cause a significant toxicity reaction against J774.A1 macrophages. With further studies, the hybrid nanoparticles MOF-PHO<sub>(67)</sub>U<sub>(7)</sub>SO<sub>3</sub><sup>-</sup>(<sub>20</sub>)PEG<sub>(6)</sub> and MOF-PHO<sub>(67)</sub>SO<sub>3</sub><sup>-</sup>(<sub>20</sub>)PEG<sub>(13)</sub> with a diameter close to 300 nm that are stable for at least 6 h in a buffered physiological environment, would constitute a new generation of biocompatible therapeutic nanovectors as innovative drug delivery system.

### AUTHOR INFORMATION

#### Acknowledgments

The Authors would like to thank Eric LEROY and Remy PIRES for their technical assistance with the SEM-STEM EDX, Annick JACQ for the access to the ClarioSTAR system and Laurent MICHELY for his technical experiment. We are grateful to the financial support of IFREMER and Region Bretagne, France.

Corresponding author

Valérie LANGLOIS

E mail: langlois@icmpe.cnrs.fr

367 **References**

- 368 (1) Anderson, A. J.; Dawes, E. A. Occurrence, metabolism, metabolic role, and industrial uses  
369 of bacterial polyhydroxyalkanoates. *Microbiol. Rev.* **1990**, *54* (4), 450–472.
- 370 (2) Steinbüchel, A.; Valentin, H. E. Diversity of bacterial polyhydroxyalkanoic acids. *FEMS*  
371 *Microbiol. Lett.* **1995**, *128* (3), 219–228.
- 372 (3) Zinn, M.; Witholt, B.; Egli, T. Occurrence, synthesis and medical application of bacterial  
373 polyhydroxyalkanoate. *Adv. Drug Deliv. Rev.* **2001**, *53* (1), 5–21.
- 374 (4) Bedian, L.; Villalba-Rodríguez, A. M.; Hernández-Vargas, G.; Parra-Saldivar, R.; Iqbal,  
375 H. M. N. Bio-based materials with novel characteristics for tissue engineering applications – a  
376 review. *Int. J. Biol. Macromol.* **2017**, *98*, 837–846.
- 377 (5) Shrivastav, A.; Kim, H.-Y.; Kim, Y.-R. Advances in the applications of  
378 polyhydroxyalkanoate nanoparticles for novel drug delivery system. *BioMed Res. Int.* **2013**,  
379 *2013*, 1–12.
- 380 (6) Li, Z.; Loh, X. J. Recent advances of using polyhydroxyalkanoate-based Nanovehicles as  
381 therapeutic delivery carriers. *Wiley Interdiscip. Rev. Nanomed. Nanobiotechnol.* **2016**, *9* (3),  
382 e1429.
- 383 (7) Zhang, J.; Shishatskaya, E. I.; Volova, T. G.; da Silva, L. F.; Chen, G.-Q.  
384 Polyhydroxyalkanoates (PHA) for therapeutic applications. *Mater. Sci. Eng. C* **2018**, *86*, 144–  
385 150.
- 386 (8) Nigmatullin, R.; Thomas, P.; Lukasiewicz, B.; Puthussery, H.; Roy, I.  
387 Polyhydroxyalkanoates, a family of natural polymers, and their applications in drug delivery.  
388 *J. Chem. Technol. Biotechnol.* **2015**, *90* (7), 1209–1221.
- 389 (9) Martin, D. P.; Williams, S. F. Medical applications of poly-4-hydroxybutyrate: a strong  
390 flexible absorbable biomaterial. *Biochem. Eng. J.* **2003**, *16* (2), 97–105.
- 391 (10) Philip, S.; Keshavarz, T.; Roy, I. Polyhydroxyalkanoates: biodegradable polymers with a  
392 range of applications. *J. Chem. Technol. Biotechnol.* **2007**, *82* (3), 233–247.
- 393 (11) Ramier, J.; Boudierlique, T.; Stoilova, O.; Manolova, N.; Rashkov, I.; Langlois, V.;  
394 Renard, E.; Albanese, P.; Grande, D. Biocomposite scaffolds based on electrospun poly(3-  
395 hydroxybutyrate) nanofibers and electrosprayed hydroxyapatite nanoparticles for bone tissue  
396 engineering applications. *Mater. Sci. Eng. C* **2014**, *38*, 161–169.
- 397 (12) Lemechko, P.; Renard, E.; Volet, G.; Colin, C. S.; Guezennec, J.; Langlois, V.  
398 Functionalized oligoesters from poly(3-hydroxyalkanoate)s containing reactive end group for

- 1  
2  
3 399 click chemistry: application to novel copolymer synthesis with poly(2-methyl-2-oxazoline).  
4  
5 400 *React. Funct. Polym.* **2012**, *72* (2), 160–167.
- 6  
7 401 (13) Alcantar, N. A.; Aydil, E. S.; Israelachvili, J. N. Polyethylene glycol-coated biocompatible  
8  
9 402 surfaces. *J. Biomed. Mater. Res.* **2000**, *51* (3), 343–351.
- 10  
11 403 (14) Lutz, J.-F. Polymerization of oligo(ethylene glycol) (meth)acrylates: toward new  
12  
13 404 generations of smart biocompatible materials. *J. Polym. Sci. Part Polym. Chem.* **2008**, *46* (11),  
14  
15 405 3459–3470.
- 16  
17 406 (15) Zalipsky, S. Synthesis of an end-froup functionalized polyethylene glycol-lipid conjugate  
18  
19 407 for preparation of polymer-grafted liposomes. *Bioconjug. Chem.* **1993**, *4*, 296–299.
- 20  
21 408 (16) He, X.; Li, L.; Su, H.; Zhou, D.; Song, H.; Wang, L.; Jiang, X. Poly(ethylene glycol)-  
22  
23 409 block-poly( $\epsilon$ -caprolactone)–and phospholipid-based stealth nanoparticles with enhanced  
24  
25 410 therapeutic efficacy on murine breast cancer by improved intracellular drug delivery. *Int. J.*  
26  
27 411 *Nanomedicine* **2015**, *10*, 1791–1804.
- 28  
29 412 (17) Lu, X.-Y.; Li, M.-C.; Zhu, X.-L.; Fan, F.; Wang, L.-L.; Ma, J.-G. Microbial synthesized  
30  
31 413 biodegradable PHBHHxPEG hybrid copolymer as an efficient intracellular delivery nanocarrier  
32  
33 414 for kinase inhibitor. *BMC Biotechnol.* **2014**, *14* (1), 1.
- 34  
35 415 (18) Shah, M.; Ullah, N.; Choi, M. H.; Kim, M. O.; Yoon, S. C. Amorphous amphiphilic  
36  
37 416 P(3HV-Co-4HB)-b-MPEG block copolymer synthesized from bacterial copolyester via melt  
38  
39 417 transesterification: nanoparticle preparation, cisplatin-loading for cancer therapy and *in vitro*  
40  
41 418 evaluation. *Eur. J. Pharm. Biopharm.* **2012**, *80* (3), 518–527.
- 42  
43 419 (19) Babinot, J.; Renard, E.; Langlois, V. Preparation of *clickable* poly(3-hydroxyalkanoate)  
44  
45 420 (PHA): application to poly(ethylene glycol) (PEG) graft copolymers synthesis. *Macromol.*  
46  
47 421 *Rapid Commun.* **2010**, *31* (7), 619–624.
- 48  
49 422 (20) Babinot, J.; Renard, E.; Langlois, V. Controlled synthesis of well defined poly(3-  
50  
51 423 hydroxyalkanoate)s-based amphiphilic diblock copolymers using click chemistry. *Macromol.*  
52  
53 424 *Chem. Phys.* **2011**, *212* (3), 278–285.
- 54  
55 425 (21) Babinot, J.; Guigner, J.-M.; Renard, E.; Langlois, V. A micellization study of medium  
56  
57 426 chain length poly(3-hydroxyalkanoate)-based amphiphilic diblock copolymers. *J. Colloid*  
58  
59 427 *Interface Sci.* **2012**, *375* (1), 88–93.
- 60 428 (22) Babinot, J.; Guigner, J.-M.; Renard, E.; Langlois, V. Poly(3-hydroxyalkanoate)-derived  
429  
430 429 amphiphilic graft copolymers for the design of polymersomes. *Chem. Commun.* **2012**, *48* (43),  
431  
432 430 5364-5366.
- 431 (23) Hazer, D. B.; Kılıçay, E.; Hazer, B. Poly(3-hydroxyalkanoate)s: diversification and  
432  
432 432 biomedical applications: a state of the art review. *Mater. Sci. Eng. C* **2012**, *32* (4), 637–647.

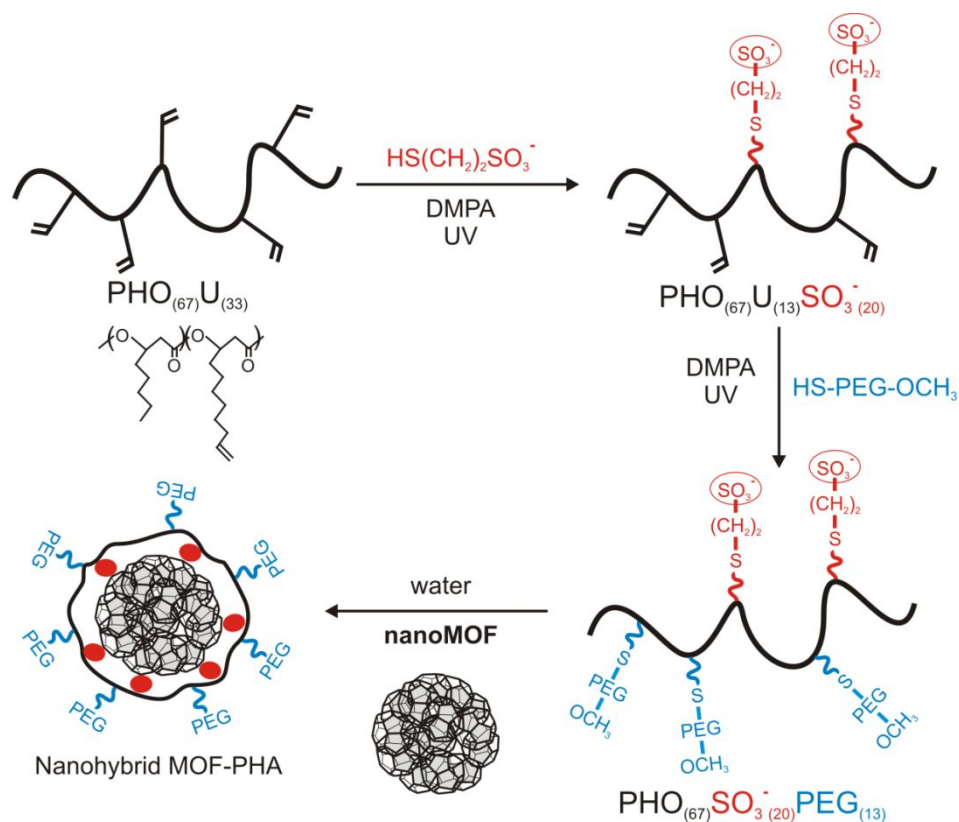
- 1  
2  
3 433 (24) Hazer, B.; Steinbüchel, A. Increased diversification of polyhydroxyalkanoates by  
4 434 modification reactions for industrial and medical applications. *Appl. Microbiol. Biotechnol.*  
5 435 **2007**, *74* (1), 1–12.
- 6  
7  
8 436 (25) Winnacker, M.; Rieger, B. Copolymers of polyhydroxyalkanoates and polyethylene  
9 437 glycols: recent advancements with biological and medical significance. *Polym. Int.* **2017**, *66*  
10 438 (4), 497–503.
- 11  
12  
13 439 (26) Ravenelle, F.; Marchessault, R. H. One-step synthesis of amphiphilic diblock copolymers  
14 440 from bacterial poly([R]-3-hydroxybutyric acid). *Biomacromolecules* **2002**, *3* (5), 1057–1064.
- 15  
16  
17 441 (27) Ravenelle, F.; Marchessault, R. H. Self-assembly of Poly([R]-3-hydroxybutyric acid)-  
18 442 block-poly(ethylene glycol) diblock copolymers. *Biomacromolecules* **2003**, *4* (3), 856–858.
- 19  
20  
21 443 (28) Li, J.; Ni, X.P.; Li, X.; Tan, N.K.; Lim, C.T.; Ramakrishna, S.; Leong, K.W. Micellization  
22 444 phenomena of biodegradable amphiphilic triblock copolymers consisting of poly( $\beta$ -  
23 445 hydroxyalkanoic acid) and poly(ethylene oxide). *Langmuir* **2005**, *21* (19) 8681-8685.
- 24  
25  
26 446 (29) Kurth, N.; Renard, E.; Brachet, F.; Robic, D.; Guerin, P.; Bourbouze, R. Poly(3-  
27 447 hydroxyoctanoate) containing pendant carboxylic groups for the preparation of nanoparticles  
28 448 aimed at drug transport and release. *Polymer* **2002**, *43*, 1095–1101.
- 29  
30  
31 449 (30) Sparks, J.; Scholz, C. Synthesis and characterization of a cationic poly( $\beta$ -  
32 450 hydroxyalkanoate). *Biomacromolecules* **2008**, *9* (8), 2091–2096.
- 33  
34  
35 451 (31) Yu, L.-P.; Zhang, X.; Wei, D.-X.; Wu, Q.; Jiang, X.-R.; Chen, G.-Q. Highly efficient  
36 452 fluorescent material based on rare-earth-modified polyhydroxyalkanoates. *Biomacromolecules*  
37 453 **2019**, *9*.
- 38  
39  
40 454 (32) Modjinou, T.; Lemechko, P.; Babinot, J.; Versace, D.-L.; Langlois, V.; Renard, E. Poly(3-  
41 455 hydroxyalkanoate) sulfonate: from nanoparticles toward water soluble polyesters. *Eur. Polym.*  
42 456 *J.* **2015**, *68*, 471–479.
- 43  
44  
45 457 (33) Pavon-Djavid, G.; Gamble, L. J.; Ciobanu, M.; Gueguen, V.; Castner, D. G.; Migonney,  
46 458 V. Bioactive poly(ethylene terephthalate) fibers and fabrics: grafting, chemical  
47 459 characterization, and biological assessment. *Biomacromolecules* **2007**, *8* (11), 3317-3325.
- 48  
49  
50 460 (34) Hany, R.; Bohlen, C.; Geiger, T.; Hartmann, R.; Kawada, J.; Schmid, M.; Zinn M.;  
51 461 Marchessault, R. H. Chemical synthesis of crystalline comb polymers from olefinic medium-  
52 462 chain-length poly[3-hydroxyalkanoates]. *Macromolecules* **2004**, *32* (2), 385-389.
- 53  
54  
55 463 (35) Li, H.; Eddaoudi, M.; O’Keeffe, M.; Yaghi, O. M. Design and synthesis of an  
56 464 exceptionally stable and highly porous metal-organic framework. *Nature* **1999**, *402* (6759),  
57 465 276–279.
- 58  
59  
60

- 1  
2  
3 466 (36) Huxford, R. C.; Della Rocca, J.; Lin, W. Metal–organic frameworks as potential drug  
4 carriers. *Curr. Opin. Chem. Biol.* **2010**, *14* (2), 262–268.
- 5 467  
6 468 (37) He, C.; Liu, D.; Lin, W. Nanomedicine applications of hybrid nanomaterials built from  
7 metal–ligand coordination bonds: nanoscale metal–organic frameworks and nanoscale  
8 coordination polymers. *Chem. Rev.* **2015**, *115* (19), 11079–11108.
- 9 470  
10 471 (38) Agostoni, V.; Chalati, T.; Horcajada, P.; Willaime, H.; Anand, R.; Semiramoth, N.; Baati,  
11 T.; Hall, S.; Maurin, G.; Chacun, H. Towards an improved anti-HIV activity of NRTI via metal-  
12 organic frameworks nanoparticles. *Adv. Healthc. Mater.* **2013**, *2* (12), 1630–1637.
- 13 473  
14 474 (39) Chalati, T.; Horcajada, P.; Couvreur, P.; Serre, C.; Ben Yahia, M.; Maurin, G.; Gref, R.  
15 Porous metal organic framework nanoparticles to address the challenges related to busulfan  
16 encapsulation. *Nanomed.* **2011**, *6* (10), 1683–1695.
- 17 476  
18 477 (40) Férey, G.; Mellot-Draznieks, C.; Serre, C.; Millange, F.; Dutour, J.; Surblé, S.; Margiolaki,  
19 I. A chromium terephthalate-based solid with unusually large pore volumes and surface area.  
20 *Science* **2005**, *309* (5743), 2040–2042.
- 21 479  
22 480 (41) Horcajada, P.; Gref, R.; Baati, T.; Allan, P. K.; Maurin, G.; Couvreur, P.; Férey, G.;  
23 Morris, R. E.; Serre, C. Metal–organic frameworks in biomedicine. *Chem. Rev.* **2012**, *112* (2),  
24 1232–1268.
- 25 482  
26 483 (42) Horcajada, P.; Chalati, T.; Serre, C.; Gillet, B.; Sebrie, C.; Baati, T.; Eubank, J. F.;  
27 Heurtaux, D.; Clayette, P.; Kreuz, C.; Chang, J.S.; Hwang, Y.K.; Marsaud, V.; Bories, P.N.;  
28 Cynober, L.; Gil, S.; Férey, G.; Couvreur, P.; Gref, R. Porous metal–organic-framework  
29 nanoscale carriers as a potential platform for drug delivery and imaging. *Nat. Mater.* **2010**, *9*  
30 (2), 172–178.
- 31 487  
32 488 (43) Agostoni, V.; Horcajada, P.; Noiray, M.; Malanga, M.; Aykaç, A.; Jicsinszky, L.; Vargas-  
33 Berenguel, A.; Semiramoth, N.; Daoud-Mahammed, S.; Nicolas, V.; Martineau, C.; Taulette,  
34 F.; Vigneron, J.; Etcheberry, A.; Serre, C.; Gref, R. A “green” strategy to construct non-  
35 covalent, stable and bioactive coatings on porous MOF nanoparticles. *Sci. Rep.* **2015**, *5* (1).  
36 491  
37 492 (44) Bellido, E.; Hidalgo, T.; Lozano, M. V.; Guillevic, M.; Simón-Vázquez, R.;  
38 Santander-Ortega, M. J.; González-Fernández, Á.; Serre, C.; Alonso, M. J.; Horcajada, P.  
39 Heparin-engineered mesoporous iron metal-organic framework nanoparticles: toward stealth  
40 drug nanocarriers. *Adv. Healthc. Mater.* **2015**, *4* (8), 1246–1257.
- 41 495  
42 496 (45) Baati, T.; Njim, L.; Neffati, F.; Kerkeni, A.; Bouttemi, M.; Gref, R.; Najjar, M. F.;  
43 Zakhama, A.; Couvreur, P.; Serre, C.; Horcajada, P. In depth analysis of the *in vivo* toxicity of  
44 nanoparticles of porous iron(III) metal–organic frameworks. *Chem. Sci.* **2013**, *4* (4), 1597–  
45 1607.
- 46 499

- 1  
2  
3 500 (46) Aykaç, A.; Noiray, M.; Malanga, M.; Agostoni, V.; Casas-Solvas, J. M.; Fenyvesi, É.;  
4 501 Gref, R.; Vargas-Berenguel, A. A non-covalent “click chemistry” strategy to efficiently coat  
5 502 highly porous MOF nanoparticles with a stable polymeric shell. *Biochim. Biophys. Acta BBA -*  
6  
7 503 *Gen. Subj.* **2017**, *1861* (6), 1606–1616.
- 8  
9 504 (47) Cai, W.; Gao, H.; Chu, C.; Wang, X.; Wang, J.; Zhang, P.; Lin, G.; Li, W.; Liu, G.; Chen,  
10  
11 505 X. Engineering phototheranostic nanoscale metal–organic frameworks for multimodal  
12 506 imaging-guided cancer therapy. *ACS Appl. Mater. Interfaces* **2017**, *9* (3), 2040–2051.
- 13  
14 507 (48) Hidalgo, T.; Giménez-Marqués, M.; Bellido, E.; Avila, J.; Asensio, M. C.; Salles, F.;  
15  
16 508 Lozano, M. V.; Guillevic, M.; Simón-Vázquez, R.; González-Fernández, A.; Serre, C.; Alonso,  
17  
18 509 M. J.; Horcajada, P. Chitosan-coated mesoporous MIL-100(Fe) nanoparticles as improved bio-  
19  
20 510 compatible oral nanocarriers. *Sci. Rep.* **2017**, *7*, 43099.
- 21  
22 511 (49) Liang, X.-X.; Wang, N.; Qu, Y.-L.; Yang, L.-Y.; Wang, Y.-G.; Ouyang, X.-K. Facile  
23  
24 512 preparation of metal-organic framework (MIL-125)/chitosan beads for adsorption of Pb(II)  
25  
26 513 from aqueous solutions. *Molecules* **2018**, *23* (7), 1524.
- 27  
28 514 (50) Wuttke, S.; Braig, S.; Preiß, T.; Zimpel, A.; Sicklinger, J.; Bellomo, C.; O. Rädler, J.;  
29  
30 515 M. Vollmar, A.; Bein, T. MOF nanoparticles coated by lipid bilayers and their uptake by cancer  
31  
32 516 cells. *Chem. Commun.* **2015**, *51* (87), 15752–15755.
- 33  
34 517 (51) Filippousi, M.; Turner, S.; Leus, K.; Sifaka, P. I.; Tseligka, E. D.; Vandichel, M.; Nanaki,  
35  
36 518 S. G.; Vizirianakis, I. S.; Bikiaris, D. N.; Van Der Voort, P. Biocompatible Zr-based nanoscale  
37  
38 519 MOFs coated with modified poly( $\epsilon$ -caprolactone) as anticancer drug carriers. *Int. J. Pharm.*  
39  
40 520 **2016**, *509* (1–2), 208–218.
- 41  
42 521 (52) Giménez-Marqués, M.; Bellido, E.; Berthelot, T.; Simón-Yarza, T.; Hidalgo, T.;  
43  
44 522 Simón-Vázquez, R.; González-Fernández, Á.; Avila, J.; Asensio, M. C.; Gref, R.; Couvreur, P.;  
45  
46 523 Serre, C.; Horcajada, P. GraftFast surface engineering to improve MOF nanoparticles  
47  
48 524 furtiveness. *Small* **2018**, *18011900*, 1–11.
- 49  
50 525 (53) Rivas, B. L.; Pereira, E. D.; Moreno-Villoslada, I. Water-soluble polymer-metal ion  
51  
52 526 interactions. *Prog. Polym. Sci.* **2003**, *28*, 173–208.
- 53  
54 527 (54) Yue, J.; Wang, Z. H.; Cromack, K. R.; Epstein, A. J.; MacDiarmid, A. G. Effect of sulfonic  
55  
56 528 acid group on polyaniline backbone. *J. Am. Chem. Soc.* **1991**, *113* (7), 2665–2671.
- 57  
58 529 (55) Babinot, J.; Renard, E.; Le Droumaguet B., ; Guigner, J.-M.; Mura S.; Nicolas J. ;  
59  
60 530 Couvreur P.; Langlois, V. Facile Synthesis of Multicompartment Micelles Based on  
531  
532 531 Biocompatible Poly(3-hydroxyalkanoate). *Macromol. Rapid Commun.* **2012**, *34*, 362-368.
- 533  
534 532 (56) Lam, J.; Herant, M.; Dembo, M.; Heinrich, V. Baseline mechanical characterization of  
535  
536 533 J774 macrophages. *Biophys. J.* **2009**, *96* (1), 248–254.

534 (57) Jenkins, S. J.; Ruckerl, D.; Cook, P. C.; Jones, L. H.; Finkelman, F. D.; Rooijen, N. van;  
 535 MacDonald, A. S.; Allen, J. E. Local macrophage proliferation, rather than recruitment from  
 536 the blood, is a signature of TH2 inflammation. *Science* **2011**, 332 (6035), 1284–1288.

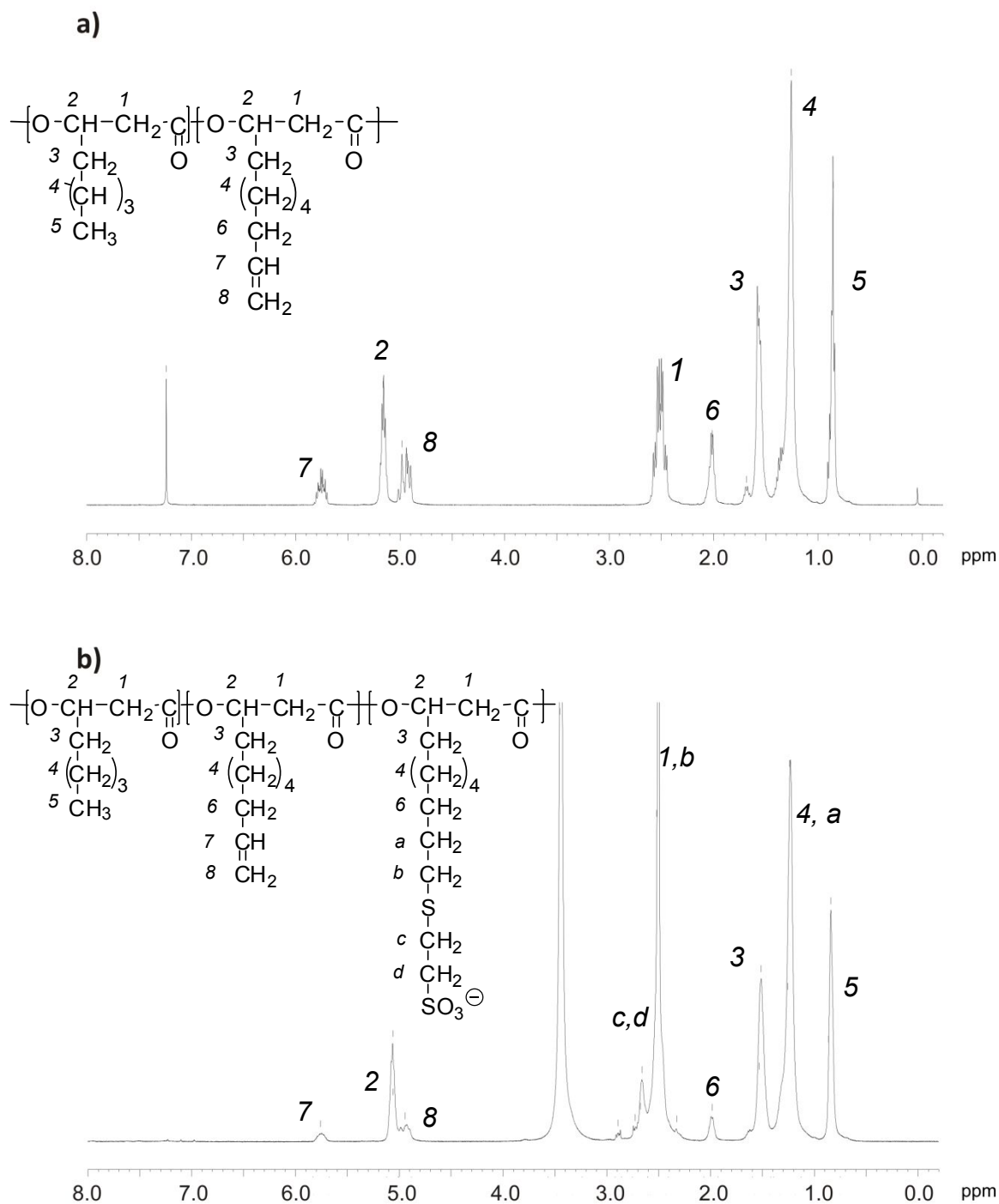
537 (58) Röszer, T. Understanding the mysterious M2 macrophage through activation markers and  
 538 effector mechanisms. *Mediators Inflamm.* **2015**, 816460.



539

540

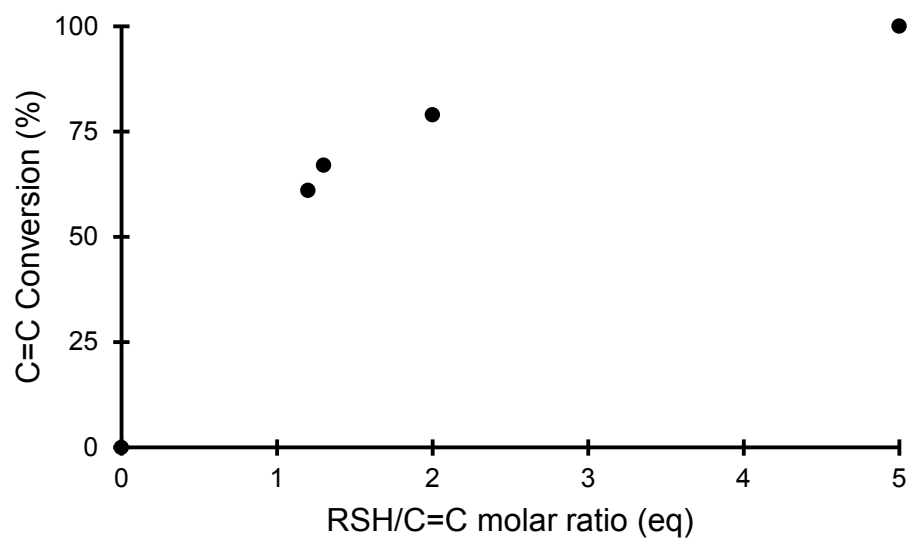
**Figure 1.** Elaboration of nanohybrid MOF-PHA



541

542 **Figure 2.**  $^1\text{H}$  NMR spectra. (a)  $\text{PHO}_{(67)}\text{U}_{(33)}$  in  $\text{CDCl}_3$  (b)  $\text{PHO}_{(67)}\text{U}_{(13)}\text{SO}_3^-(20)$  in  $\text{DMSO-d}_6$

543

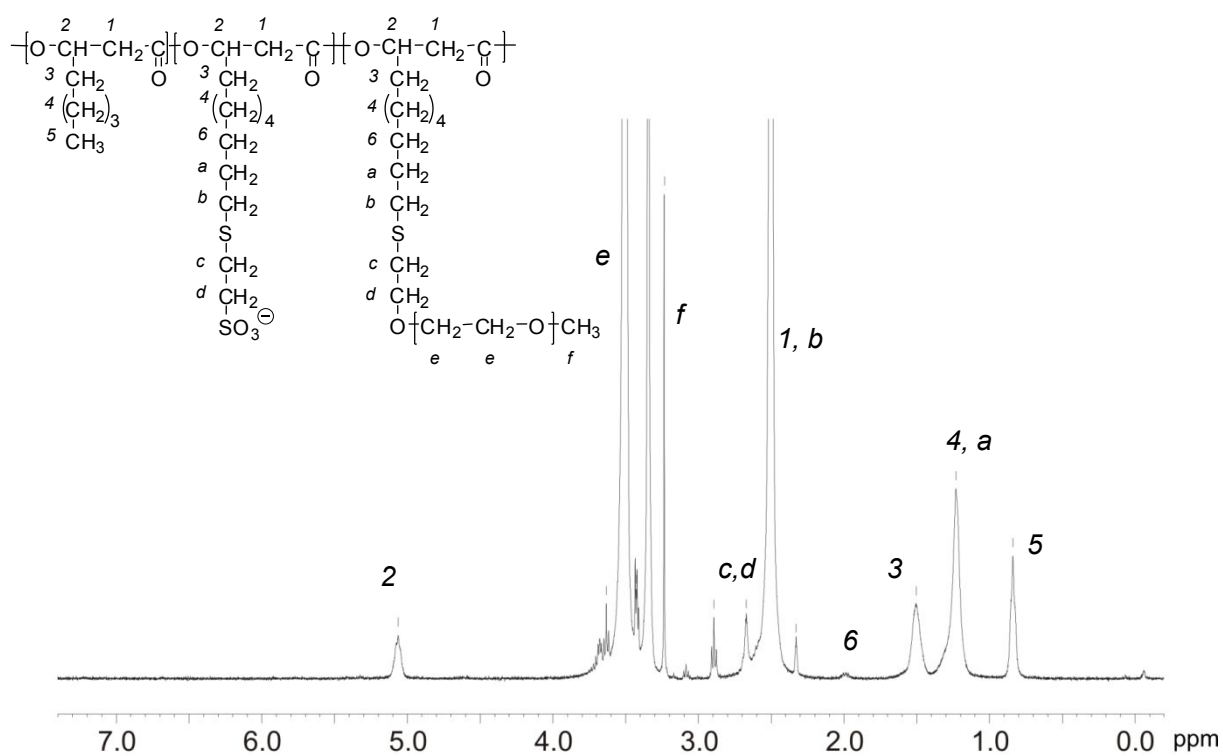


544

545

**Figure 3.** C=C conversion of  $\text{PHO}_{(67)}\text{U}_{(33)}$  determined by  $^1\text{H}$  NMR

546



547

548

**Figure 4.**  $^1\text{H}$  NMR spectrum of  $\text{PHO}_{(67)}\text{SO}_3^-(20)\text{PEG}_{(13)}$  in  $\text{DMSO-d}_6$ .

549

550

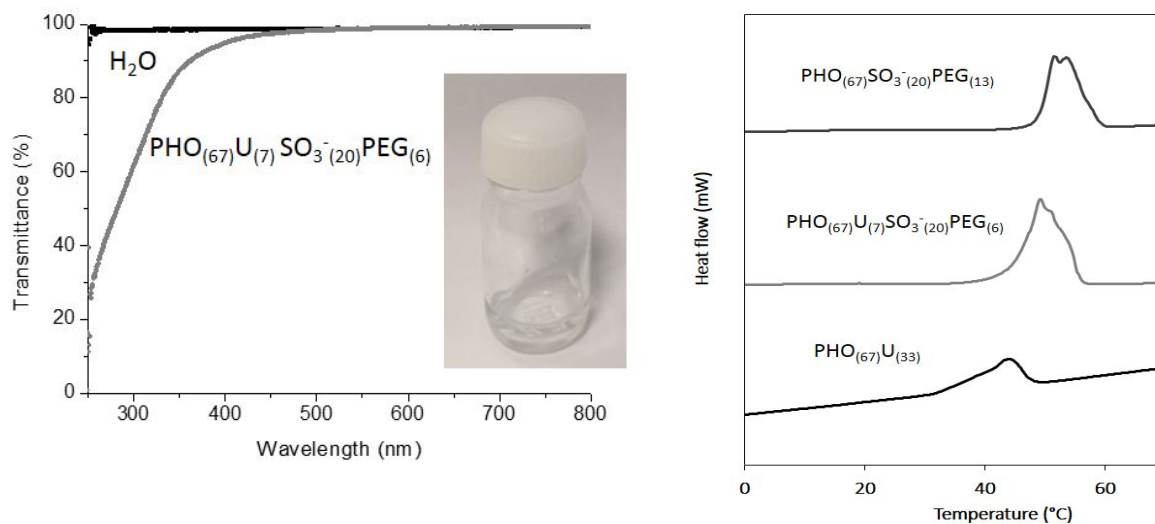
551

552

553

554

555

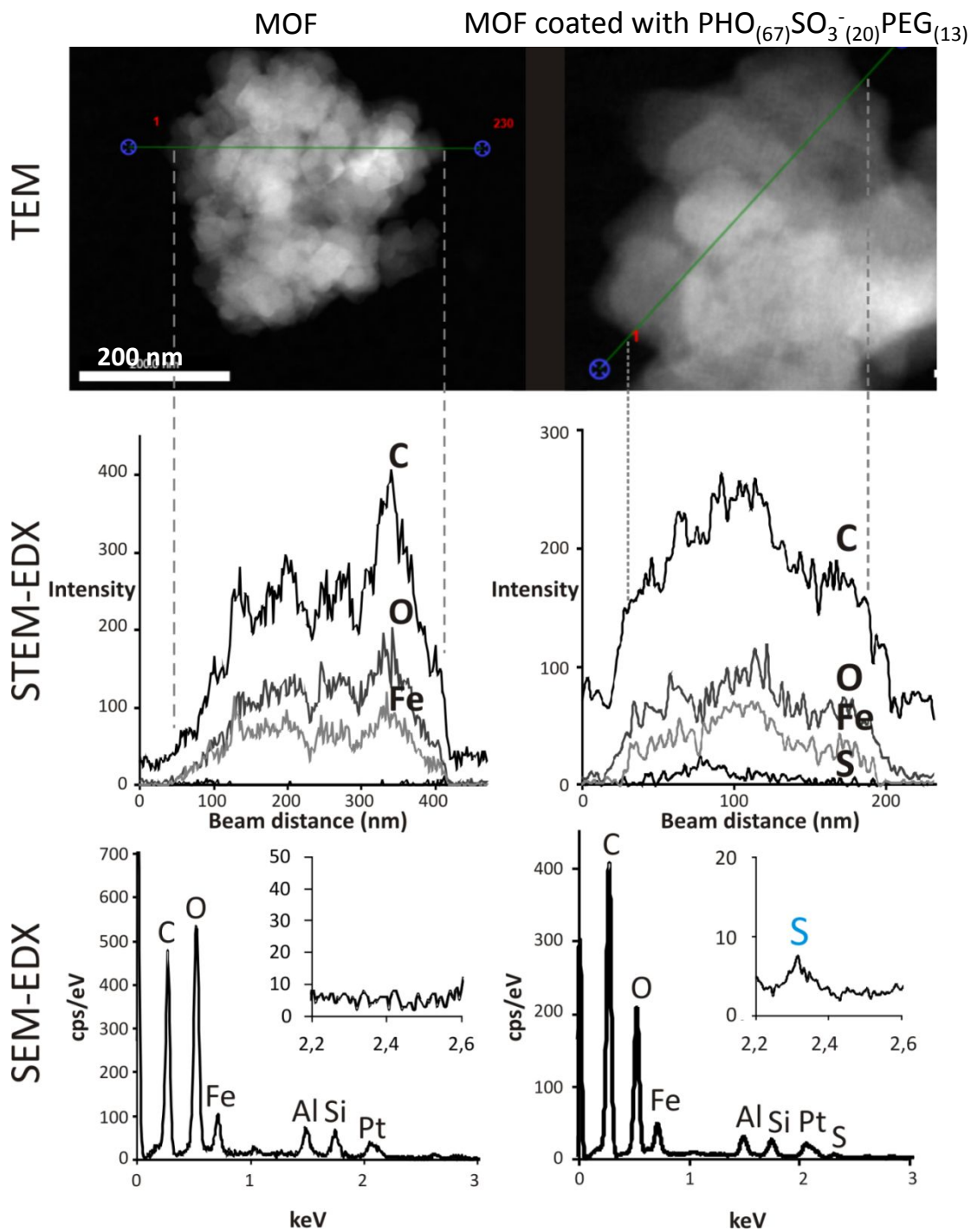


556

557 **Figure 5.** Transmittance measurements in ultrapure water and DSC curves. Only the first  
558 heating is reported.

559

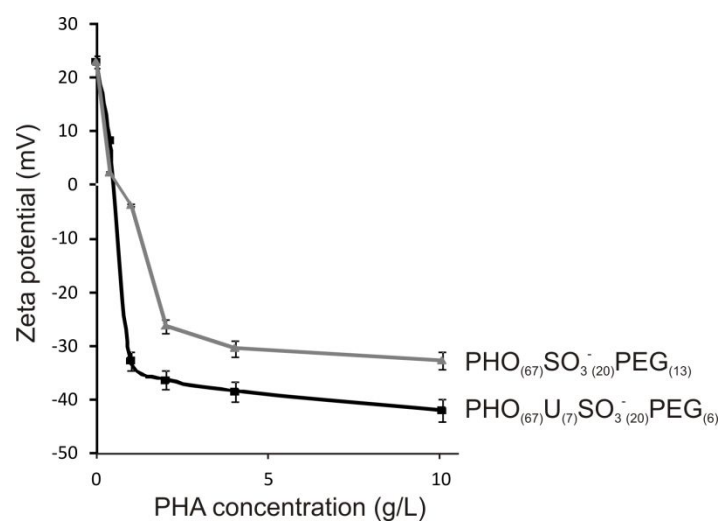
560



561

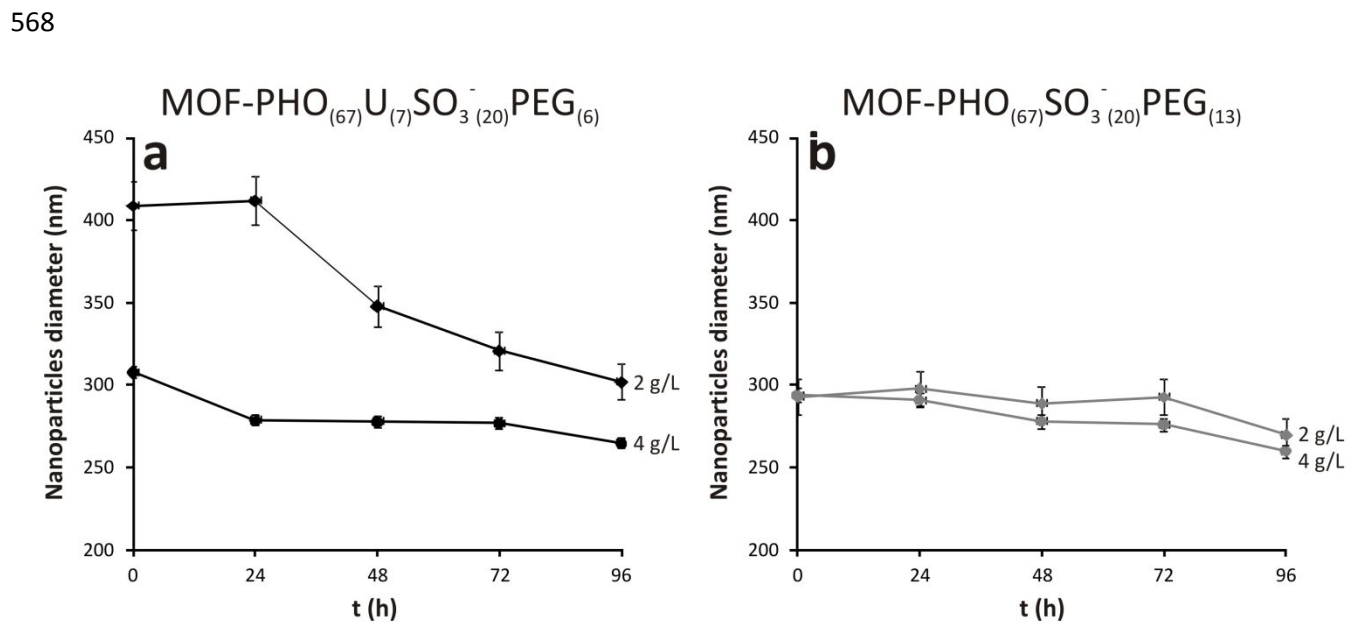
562 **Figure 6.** TEM, STEM-EDX and SEM-EDX analysis of free MOF nanoparticles and coated563 with  $\text{PHO}_{(67)}\text{SO}_3^-(20)\text{PEG}_{(13)}$

564

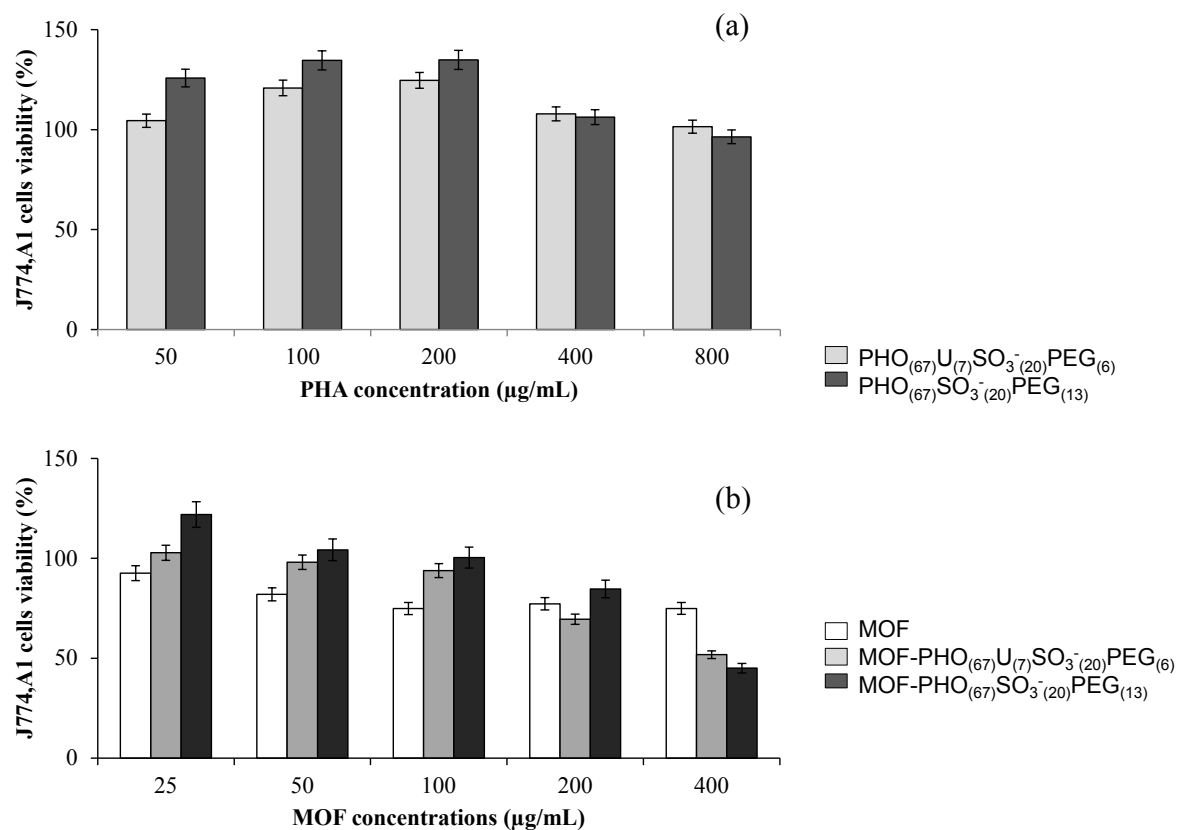


565

566 **Figure 7.** Zeta potential of MOF nanoparticles coated with  $\text{PHO}_{(67)}\text{SO}_3(20)\text{PEG}_{(13)}$  and  
567  $\text{PHO}_{(67)}\text{U}_{(7)}\text{SO}_3(20)\text{PEG}_{(6)}$

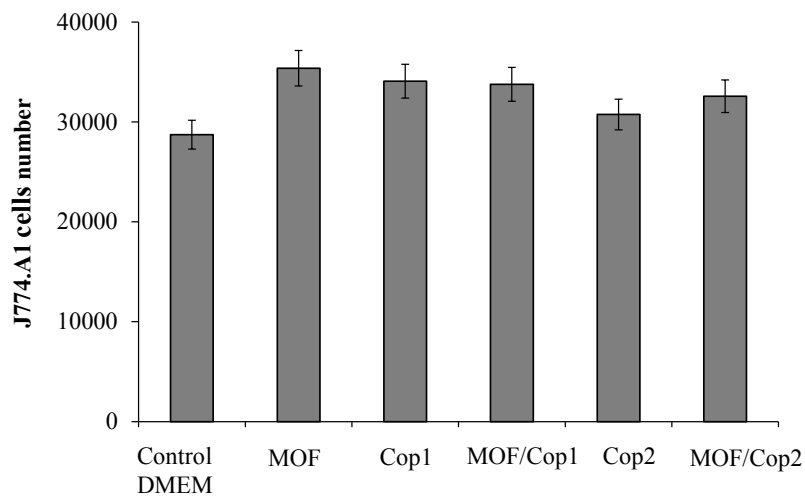


23 569 **Figure 8.** MOF-PHA hybrid nanoparticles diameters measured for 96 h in ultra pure water at  
24 different copolymer concentrations.  
25 570



571

572 **Figure 9.** Viability of J774.A1 cells calculated using an LDH test, as a function of the  
 573 concentrations of copolymers (a) or nanoMOFs, native or coated with functionalized PHA (b),  
 574 after 24 hours of incubation. DMEM was used as control (100%). Experiments were done in  
 575 triplicate.



576

577 **Figure 10.** Number of viable J774.A1 cells determined by the RealTime Glo test for 42 h in  
578 presence of MOF and coated MOF by  $\text{PHO}_{(67)}\text{U}_{(7)}\text{SO}_3^-(20)\text{PEG}_{(6)}$  noted Cop1 or  $\text{PHO}_{(67)}\text{SO}_3^-$   
579  $(20)\text{PEG}_{(13)}$  noted Cop2

1  
2  
3 580  
4  
5  
6 581  
7 582  
8  
9 583

**Table 1.** Characterization of PEG, PHO<sub>(67)</sub>U<sub>(33)</sub>, PHO<sub>(67)</sub>U<sub>(7)</sub>SO<sub>3</sub><sup>-</sup><sub>(20)</sub>PEG<sub>(6)</sub> and PHO<sub>(67)</sub>SO<sub>3</sub><sup>-</sup><sub>(20)</sub>PEG<sub>(13)</sub> polymers.

Samples	Molar masses		Thermal properties			
	Mn (g/mol)	PDI	Tg <sup>c</sup> (°C)	Tm <sup>d</sup> (°C)	ΔHm <sup>d</sup> (J/g)	
					PHA	PEG
PEG <sub>2000</sub>	1,700 <sup>b</sup>	1.3 <sup>b</sup>	-	53	-	185
PHO <sub>(67)</sub> U <sub>(33)</sub>	40,000 <sup>a</sup>	1.7 <sup>a</sup>	-40	44	14	-
PHO <sub>(67)</sub> U <sub>(7)</sub> SO <sub>3</sub> <sup>-</sup> <sub>(20)</sub> PEG <sub>(6)</sub>	24,000 <sup>b</sup>	1.1 <sup>b</sup>	-	49	-	82
PHO <sub>(67)</sub> SO <sub>3</sub> <sup>-</sup> <sub>(20)</sub> PEG <sub>(13)</sub>	29,500 <sup>b</sup>	1.1 <sup>b</sup>	-	52	-	132

23 584  
24 585  
25 586  
26 587  
27 588  
28 589  
29 590  
30  
31  
32  
33  
34  
35  
36  
37  
38  
39  
40  
41  
42  
43  
44  
45  
46  
47  
48  
49  
50  
51  
52  
53  
54  
55  
56  
57  
58  
59  
60

<sup>a</sup> Determined by SEC in CHCl<sub>3</sub>.

<sup>b</sup> Determined by SEC in H<sub>2</sub>O/LiNO<sub>3</sub>

<sup>c</sup> Recorded from the second heating of DSC.

<sup>d</sup> Recorded from the first heating of DSC, for copolymers ΔHm was calculated using the formula  $\Delta H = \Delta H_i / W_i$ , where ΔH<sub>i</sub> is the area of the DSC endothermic peak, and W<sub>i</sub> is the weight of PHA or PEG determined by <sup>1</sup>H RMN.

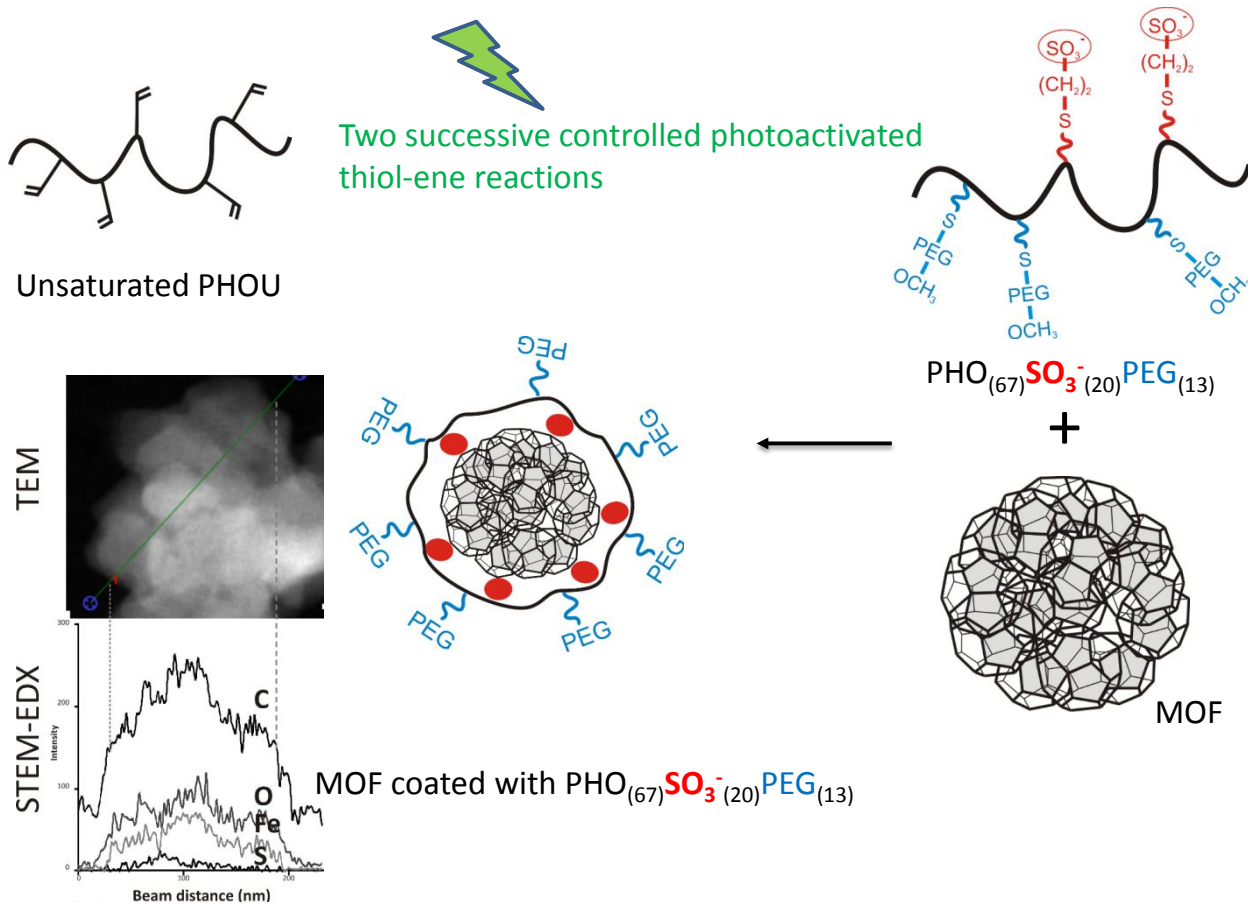
1  
2  
3 591  
4 592  
5  
6 593  
7 594  
8  
9 595  
10  
11

**Table 2.** Average atomic composition of MOF nanoparticles determined by STEM or SEM-EDX

Nanoparticles		C (%)	O (%)	Fe (%)	S (%)	Ratio C/Fe	Ratio S/Fe
STEM-EDX	MOF	74.6	18.8	6.4	0.0	11.6	0.00
	MOF- PHO <sub>(67)</sub> U <sub>(7)</sub> SO <sub>3</sub> <sup>-</sup> <sub>(20)</sub> PEG <sub>(6)</sub>	76.7	16.6	5.9	0.8	12.9	0.13
	MOF- PHO <sub>(67)</sub> SO <sub>3</sub> <sup>-</sup> <sub>(20)</sub> PEG <sub>(13)</sub>	77.7	16.4	5.2	0.8	15.1	0.16
SEM-EDX	MOF	55.2	38.3	6.5	0.0	8.5	0.00
	MOF- PHO <sub>(67)</sub> U <sub>(7)</sub> SO <sub>3</sub> <sup>-</sup> <sub>(20)</sub> PEG <sub>(6)</sub>	69.2	23.0	6.9	0.9	10.0	0.13
	MOF- PHO <sub>(67)</sub> SO <sub>3</sub> <sup>-</sup> <sub>(20)</sub> PEG <sub>(13)</sub>	70.0	22.9	6.3	0.8	11.1	0.13

26 596  
27  
28  
29  
30 597  
31  
32  
33 598  
34  
35  
36 599  
37  
38  
39 600  
40  
41  
42 601  
43  
44  
45  
46  
47  
48  
49  
50  
51  
52  
53  
54  
55  
56  
57  
58  
59  
60

## 602 Table of Contents graphic



603